Short communication

Study of the polarizable centers in single crystal dolomite $(CaMg(CO_3)_2)$ rich in Fe^{3+} impurities by thermally stimulated depolarization current spectroscopy

A.N. Papathanassiou*

Section of Solid State Physics, Department of Physics, University of Athens, Panepistimiopolis, GR 157 84, Zografos, Athens, Greece

Abstract

Trivalent iron cations show a strong preference for substituting the magnesium cations of the mixed crystal dolomite. In the present work, we identify dielectric relaxation mechanisms, which correspond to different dipole defect configuration and investigate their dynamics by employing thermally stimulated depolarization current technique. A selective polarization scheme was successfully employed to resolve different mechanisms, which overlap strongly. Two dominant relaxations are located at 205 and 247 K, respectively, and are related to the presence of iron in the dolomite matrix. The signals were analyzed assuming a normal distribution in the activation energy values. Different dipole defect configurations are discussed.
© 2002 Elsevier Science Ltd. All rights reserved.

Keywords: C. Ionic thermocurrent; D. Dielectric properties

1. Introduction

Dolomite $(CaMg(CO_3)_2)$ is a mixed crystal with calcite $(CaCO_3)$ and magnesite $(MgCO_3)$ as its end members. Calcite, magnesite and dolomite constitute the rhombo-herdral calcite group and may be approximated to sodium chloride structure provided that the cubic unit cell is suppressed along its diagonal axis [1]. Within this visualization, the divalent cation replaces the sodium anion and the carbonate group replaces the chlorine ion. However, the carbonate group is not a center of symmetry, since the three oxygens in magnesite and calcite settle at the corners of an equilateral triangle, and the carbon is located at its center [2]. Slight distortions and deviations from the aforementioned picture preserve the structural stability of dolomite [2].

A series of papers on the dielectric properties of the calcite group materials has been published during the past years [3–8]. The scope was to investigate the role of the lattice parameters on the formation of dipole defects and

their rotational dynamics. [3,4,6]. These dipole defects are composed of impurity ions and aliovalent cation vacancies [4]. For example, in calcite, Sr^{2+} impurities are positioned in interstitial sites. The extra electric charge ($2|e|$; e is the electron's electric charge) is compensated by the creation of a calcium vacancy with effective electric charge $-2|e|$. The mutual electrostatic attraction of the Sr^{2+} cations and the calcium vacancy yields a dipole defect. The mixing of two ionic systems giving rise to a new mixed crystal induces long and short-range effects, which influence the dynamics of the dipole defects [9]. The long-range effect is related to the modification of the lattice spacing resulting from the mixing. The short-range effect results from the modification of the immediate environment of the rotating dipole [9]. By using the thermally stimulated depolarization current (TSDC) spectroscopy [10], we found that two different relaxation mechanisms occur in the members of the calcite family [3]. One is favored in the magnesium sub-lattice and is related to the rotation of dipoles consisting of hydroxyls which are characterized as strongly bound to the matrix since they cannot be removed from the bulk after heating the crystal at

---

* Fax: +30-107661707.
E-mail address: apapathan@in.gr (A.N. Papathanassiou).

elevated temperature (anneal). The other one is related to the rotation of defect clusters with Sr^{2+} as the most important participant [3,7].

The question on the distribution of paramagnetic ions, like Mn^{2+} and Fe^{3+} on different sites of dolomite has been investigated by electron paramagnetic resonance [11]. Both ions exhibit a strong preference for replacing Mg ions. The accommodation of Mn^{2+}, which is much larger than Mg^{2+}, results in slight distortions in the lattice. On the other hand, Fe^{3+} does not significantly mismatch the Mg site, but the extra positive electric charge requires a charge compensation configuration. EPR studies on the same crystal (i.e. dolomite with a considerable content of iron) [11], indicated that the excess charge is compensated locally by the exchange on the threefold axis of one carbon ion by boron. The bonding between the carbon or the boron and the three oxygens of the carbonate group is dominantly covalent, while the nature of the carbonate trioxygen group-alkaline earth cations is mainly ionic. Thus, the immediate environment of boron is covalent and is embedded into an ionic matrix. However, the amount of boron is too low to account for the compensation of the total excess charge of the iron impurities. Recalling that the incorporation of divalent cation impurities in the alkali halide crystals results in the creation of cation vacancies, so as to preserve the electrical neutrality of the crystal, it is reasonable to suggest the creation of one cation vacancy (with effective charge $-2|e|$, where e denotes the electron's charge) for each pair of iron impurities. The result is the formation of agglomerates consisting of two iron impurities and a single cation vacancy. The deviation of the dolomite's structure from the cubic one, the above-mentioned double iron-cation vacancy complex would have a non-electric dipole moment. If our assertion is correct, the dielectric spectrum of dolomite rich in Fe^{3+} should exhibit two relaxation mechanisms: one corresponding to the boron–iron complex and another to the double-iron-vacancy aggregate. The experimental technique used is the TSDC spectroscopy.

2. Theory

Consider an insulator accommodating permanent electric dipoles, which consist of charged dipole defects. The rotation of such dipoles is attained by the migration of the bound defects. The dielectric relaxation is determined by the relaxation time τ, which strongly depends on the temperature. A common assumption is that the following Arrhenius equation is valid:

$$\tau(T) = \tau_0 \exp\left(\frac{E}{kT}\right) \tag{1}$$

where k is Boltzmann's constant, E denotes the activation energy and τ_0 is the pre-exponential factor. The activation energy E is identical to the enthalpy h^m for the migration of

the (bound) defect [12]. The pre-exponential factor τ_0 is directly related to the migration enthalpy s^m via the following relation [12]:

$$s^m = -k \ln(A \nu \tau_0) \tag{2}$$

where A is a geometric factor and ν is the vibrational frequency of the migrating defect. The potential energy separating two neighboring equilibrium states corresponds to the migration Gibbs energy $g^m = h^m - Ts^m$. At low temperatures (i.e. below room temperature) $g^m \cong h^m$. By using the thermodynamic definition $s^m \equiv -(\partial g^m/\partial T)_T$, we get (in the low temperature limit) the percent modification of the potential barrier for dipole rotation upon temperature:

$$\frac{s^m}{E} \cong -\frac{(\partial h^m/\partial T)_P}{h^m} = -\left(\frac{\partial \ln h^m}{\partial T}\right)_P \tag{3}$$

h^m and τ_0 may be evaluated experimentally from the analysis of the TSDC signals.

For the simple case of non-interacting rotating dipoles, the depolarization current $I(T)$ resembles a glow curve [10]:

$$I(T) = \frac{S\Pi_0}{\tau_0} \exp\left[-\frac{E}{kT} - \frac{1}{b\tau_0} \int_{T_0}^{T} \exp\left(-\frac{E}{kT}\right) dT\right] \tag{4}$$

where Π_0 is the initial polarization of the dielectric, S is the surface sample area which is in contact with each one of the electrodes, b is the heating rate, E is the activation energy of the rotating dipoles (which is identical to h^m) and T_0 coincides to the liquid nitrogen temperature (LNT). In most cases, a normal distribution of the activation energy value around E_0 holds [13,14]

$$f(E) = \frac{1}{\sqrt{2\pi}\sigma} \exp\left[-\frac{(E - E_0)^2}{2\sigma^2}\right] \tag{5}$$

where σ denotes the broadening parameter. The modified depolarization current can be written:

$$I(T) = \int_{-\infty}^{+\infty} f(E)I(T, E) dE \tag{6}$$

where the term $I(T, E)$ is the monoenergetic TSDC equation (see Eq. (4)).

3. Experimental details

The TSDC experiments were performed in a vacuum cryostat operating from the LNT to 400 K. More details are given in Ref. [7]. The natural single crystals of dolomite were from Oberdorf, Styria (Austria) and contain a considerable amount of iron. Other researchers [11,15] studied earlier the structural and spectroscopic features of the same crystal. The specimens were clear and prepared along their cleavage planes. The chemical analysis is cited in Ref. [15], in wt%: CaO 30.1, MgO 20.4, FeO 1.8, Mn? 0.5. Additional analyses in the Institute of Geological and Mining Research (IGME, Greece), gave the following
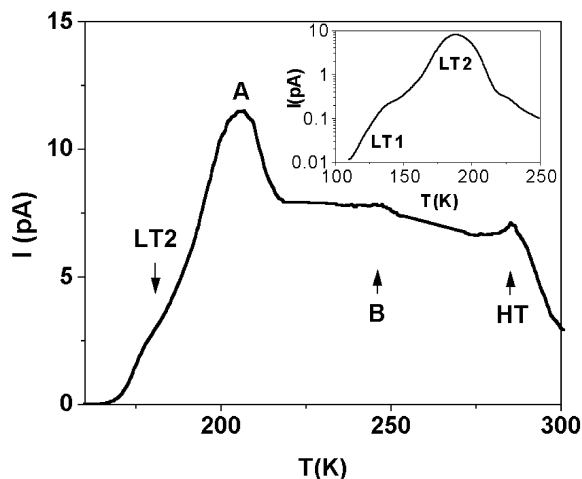
Fig. 1. A thermogram obtained by applying an electric field of intensity $E_p = 10^6$ V/m at $T_p = 290$ K for the time interval $t_p = 2$ min. Platinum electrodes were used. The heating rate was 0.033 K/s. In the inset diagram the low temperature mechanisms are depicted, by polarizing at $T_p = 190$ K (Details are given in Ref. [7]).

results, in wt%: Si 0.9, Al 0.02, Sr 0.02, K less than 0.01, Na 0.03, humidity 0.38.

4. Results and discussion

The thermogram obtained by polarizing the sample at room temperature is shown in Fig. 1. Satellite peaks surround the strong peak that reaches a maximum at 205 K. In a paper published earlier [7], the low temperature region was investigated by combined TSDC and infrared spectroscopies; two mechanisms located at 140 K (LT1 peak) and 188 K (LT2 peak) are presented in semi-logarithmic plot in the inset graph. The dominant relaxation at 205 K is labeled as A band. LT2 appears as a 'knee' in the low temperature part of the A-band (Fig. 1). At higher temperatures, a plateau-like signal follows. The 200–250 K region consists of many overlapping peaks. A visual inspection of Fig. 1 indicates that two intense mechanisms are probably cited at 247 K (B peak) and 285 K (HT peak).

Although the thermogram is too complicated to distinguish clearly between the particular relaxation components, we performed successive experiments under the same polarization conditions. The location and the amplitude of the A-peak did not change, while mechanism B showed moderate reproducibility in its amplitude. However, the last observation is potentially affected by the irreproducibility of the HT peak. Relaxation A is insensitive to the electrode material (platinum, bronze, silver paste or teflon) [16]. The reproducibility and the independence upon the electrode material are typical of dipole relaxation. Hence, it
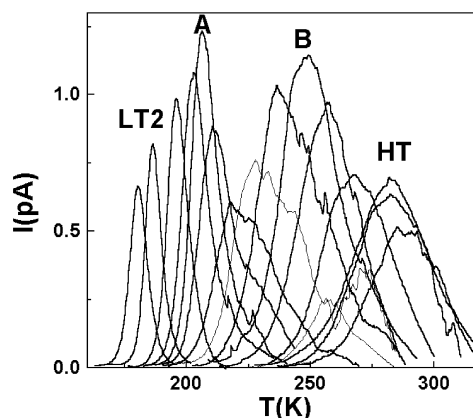

Fig. 2. Decomposition of the dielectric relaxation spectrum of single crystal dolomite to some of its constituents, by employing the selective polarization scheme.

is probable that mechanisms A and B are produced by the rotation of permanent electric dipoles. HT has the features of space charge polarization mechanism [17].

The dielectric spectrum was decomposed by employing a selective polarization scheme [7,18–20], which is an alternative of the thermal sampling technique [16]. Instead of polarizing within a temperature window [16], the polarization state is initially attained by polarizing at a constant temperature T_p (within the region where a broad dispersion occurs), for a short time interval $t_p = 1$ min. At the same temperature, the sample is subsequently discharged for the time interval $t_p = 1$ min and is afterwards quenched to the LNT in the absence of an external electric field. The polarization at T_p for a short time interval prohibits the polarization of the undesirable high temperature contributions. On the other hand, the subsequent discharge at T_p annihilates the low temperature fast relaxation mechanisms. Therefore, the selective polarization sample consists of components, which activate in the immediate neighborhood of T_p. In Fig. 2, some of the responses that build up the dielectric relaxation of dolomite are depicted. In the low temperature region, the LT1 and LT2 peaks appear clearly. Their maxima depend on the polarization temperature, indicating that their relaxation parameters are not single valued but distributed [16]. Another intense signal is located at 247 K (B mechanism), while a sub-set of signals seems to accumulate around 283 K (HT mechanism). The components of the B relaxation are affected in their high temperature tail by the contributions of the neighboring HT relaxation. The relaxation parameters of the mechanisms detected by the selective polarization are enlisted in Table 1. For the peaks attributed to mechanisms LT2 and A, Eq. (5) was fitted to the experimental data points, but, a final visual inspection yielded the theoretical curve that matched the low temperature side of the experimental peak. For the constituents of relaxations B and HT, where their end tails are noisy and suffer from

Table 1
The relaxation parameters obtained by matching a theoretical curve with normal distribution of the activation energy values to the experimental selective polarization signals

Relaxation mechanism	T_{max} (K)	E_0 (eV)	τ_0 (s)
LT2	180.3	0.571	9.50×10^{-15}
	186.3	0.581	1.78×10^{-14}
A	195.8	0.611	1.80×10^{-14}
	202.9	0.617	4.93×10^{-14}
	206.3	0.623	6.62×10^{-14}
	211.0	0.628	1.14×10^{-13}
B	217.6	0.650	1.08×10^{-13}
	227.8	0.654	4.47×10^{-13}
	236.2	0.655	1.53×10^{-12}
	248.6	0.660	6.67×10^{-12}
	256.0	0.683	5.91×10^{-12}
	267.3	0.702	1.03×10^{-11}
HT	271.8	0.755	1.71×10^{-12}
	282.0	0.780	2.03×10^{-12}
	282.1	0.790	1.34×10^{-12}
	287.0	0.771	5.61×10^{-12}
	294.4	0.780	8.66×10^{-12}

neighboring satellites, a theoretical curve was determined after a few iterations, trying to match the initial rise of the signals. The central value E_0 is plotted in Fig. 3(a) as a function of the temperature T_{max} where the peak maximum appears. The corresponding τ_0 values are depicted in Fig. 3(b). The broadening parameter σ of the activation energy distribution is represented by vertical bars in the $E_0(T_{max})$ diagram. We note that the σ values are actually suppressed when the thermal sampling is employed. Eq. (2) indicates that $-\log_{10}\tau_0$ is functioned to the migration enthalpy s^m *for dipole rotation* and, therefore, the ratio $(-\log_{10}\tau_0)/E_0$ is representative of the percentage variation of the height of the potential barriers on temperature. $(-\log_{10}\tau_0)/E_0$ vs T_{max} is depicted in Fig. 4. The physical content of the aforementioned ratio is not direct for space charge mechanisms, like the HT band, where the activation energy is the sum of the migration enthalpy for the free charge motion plus a term corresponding to the association of defects [21].

Our experiments are compared critically with the TSDC results reported for dolomite containing negligible traces of iron [4], where peaks A and B were not detected at all. Consequently, peaks A and B are related to the presence of iron in dolomite. The distribution in the activation energy values has been interpreted in the literature as a consequence of the electrostatic interaction between the dipole centers, since their density is quite high. The percentage variation of the pre-exponential factor is negligible (about 5%) compared with the uncertainty in estimating τ_0. It seems that the pre-exponential factor is rather single valued.

The appearance of two additional relaxations (A and B) when dolomite accommodates Fe^{3+} impurities indicates that two different dipole defects (involving iron cations) are
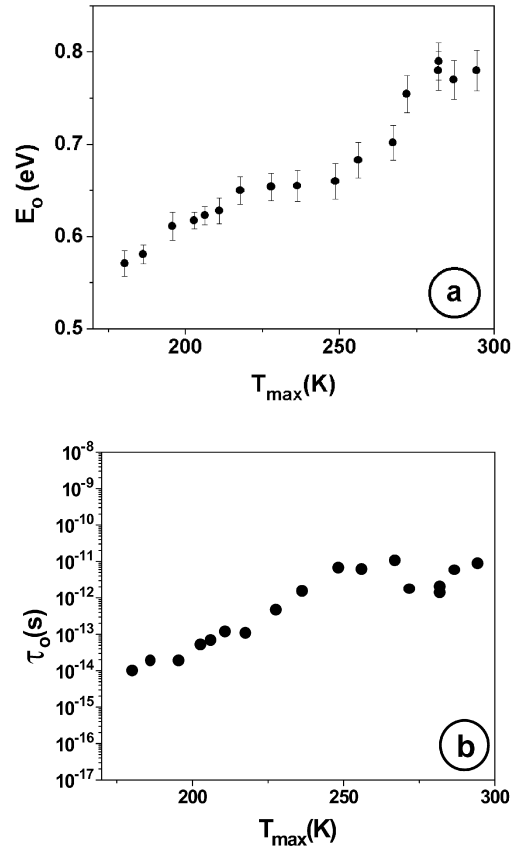

Fig. 3. (a) The central values of the activation energy E_0 and (b) the pre-exponential factor τ_0 vs the temperature T_{max} where the selective polarization signals exhibit a maximum. A Gaussian distribution in the activation energy values is asserted. The vertical bars are twice the broadening parameter σ.
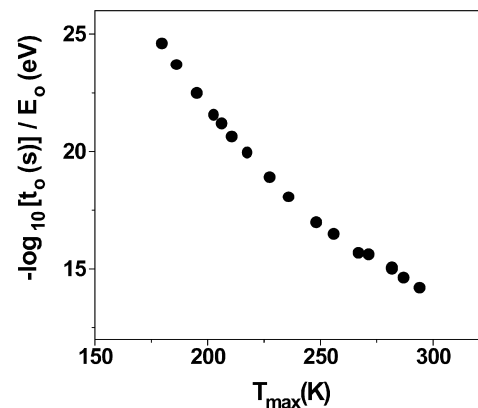

Fig. 4. The ratio $-\log_{10}\tau_0/E_0$, which (for dipole rotation) is representative of the percentage variation of the potential barriers upon temperature, as a function of the temperature T_{max} where a selective polarization signal has its maximum.

formed. The boron concentration is low enough (in comparison to the significant concentration of trivalent iron cations) to preserve the electrical neutrality of the crystal. Therefore, apart from the iron–boron complex (see Section 1) it is likely to assume that a two vacancy-iron complex is also formed. The rotation of such agglomerate should be characterized by a larger relaxation time than that of the A-mechanism. In other words, the iron–boron complex should relax faster than any larger agglomerate. Thus, the A and B bands may be attributed to the relaxation of iron–boron dipoles and double iron-cation vacancy complexes, respectively. Alternatively, relaxation B may be related with the polarization of (highly conductive) vacancy-rich islands embedded in the matrix. Within this frame, the cation vacancies formed due to the presence of iron, as well as the iron cations themselves, precipitate and form conductive territories within the (insulating) matrix. The polarization involves the localized motion of charge carriers and may be regarded as an interfacial (Maxwell Wagner) procedure. In this case, provided that the charge carriers migrate along longer distances in the conductive phase, the relaxation time should be longer than that of the iron–boron dipole, where the charge motion is too short. Subsequently, the slower relaxation mechanism (i.e. response B) should be attributed to the aforementioned interfacial phenomenon.

5. Conclusions

Employing the selective polarization scheme, the major components of the complex dielectric spectrum of dolomite with considerable concentration of iron were recorded. Two relaxations (A and B) are related to the presence of iron in the matrix and are characterized by the distribution in the activation energy values. The compensation of the extra charge induced by the incorporation of the trivalent iron cations is made in two ways: by the substitution of carbon by boron impurities and by the formation of one cation vacancy for each pair of iron impurities. The resulting dipolar centers are responsible for the appearance of bands A and B, respectively. It is also probable that peak B ir related to the interfacial polarization due to conductive vacancy and iron rich phases in dolomite.

References

[1] W.A. Deer, R.A. Howie, J. Zussman, An Introduction to the Rock Forming Minerals, Longman, Essex, 1966.

[2] R.J. Reeder, in: R.J. Reeder (Ed.), Crystal Chemistry of Rhombohedral Carbonates in Reviews in Mineralogy, Carbonates: Mineralogy and Chemistry, vol. 11, Mineralogical Society of America, Washington, 1983.

[3] A.N. Papathanassiou, J. Grammatikakis, Phys. Rev. B 56 (1997) 8590.

[4] A.N. Papathanassiou, J. Grammatikakis, Phys. Rev. B 53 (1996) 16253.

[5] N.G. Bogris, J. Grammatikakis, A.N. Papathanassiou, in: O. Kanert, J.-M. Spaeth (Eds.), Proceedings of the XII International Conference on Defects in Insulating Materials ICDIM92 (Germany, 1992), World Scientific, Singapore, 1993, p. 804.

[6] A.N. Papathanassiou, J. Grammatikakis, V. Katsika, A.B. Vassilikou-Dova, Radiat. Effects Defects Solids 134 (1995) 247.

[7] A.N. Papathanassiou, J. Grammatikakis, J. Phys. Chem. Solids 61 (2000) 1633.

[8] A.N. Papathanassiou, J. Phys. D: Appl. Phys. 34 (2001) 2825.

[9] R. Robert, R. Barboza, G.F.L. Ferreira, M. Ferreira de Souza, Phys. Stat. Sol. (b) 59 (1973) 335.

[10] C. Bucci, R. Fieschi, Phys. Rev. Lett. 12 (1964) 16.

[11] F. Prissok, G. Lehmann, Phys. Chem. Miner. 13 (1986) 331.

[12] P.A. Varotsos, K.D. Alexopoulos, in: S. Amelinckx, R. Gevers, J. Nihoul (Eds.), Thermodynamics of Point Defects and their Relation with Bulk Properties, North-Holland, Amsterdam, 1985.

[13] J.P. Calame, J.J. Fontanella, M.C. Wintersgill, C. Andeen, J. Appl. Phys. 58 (1985) 2811.

[14] E. Laredo, M. Puma, N. Suarez, D.R. Figueroa, Phys. Rev. B 23 (1981) 3009.

[15] H. Effenberger, K. Mereiter, J. Zemann, Zeischrift fur Kristallographie 156 (1981) 233.

[16] J. Vanderschueren, J. Gasiot, in: P. Braunlich (Ed.), Field Induced Thermally Stimulated Currents in Thermally Stimulated Relaxation in Solids, Springer, Berlin, 1979.

[17] J. van Turnhout, in: G.M. Sessler (Ed.), Thermally Stimulated Discharge of Polymers in Electrets, Springer, Berlin, 1980.

[18] A.N. Papathanassiou, J. Phys. Chem. Solids 60 (1999) 407.

[19] A.N. Papathanassiou, J. Grammatikakis, Phys. Rev. B 61 (2000) 16514.

[20] A.N. Papathanassiou, J. Phys. Condensed Matter 12 (2000) 5789.

[21] Da.Yu. Wang, A.S. Nowick, Phys. Stat. Sol. (a) 73 (1982) 165.